

1 **Potential of surrogate modelling for probabilistic fire analysis of structures**

2 Ranjit Kumar Chaudhary, Ruben Van Coile & Thomas Gernay

3 **ABSTRACT**

4 The interest in probabilistic methodologies to demonstrate structural fire safety has increased
5 significantly in recent times. However, the evaluation of the structural behavior under fire
6 loading is computationally expensive even for simple structural models. In this regard, machine
7 learning-based surrogate modeling provides an appealing way forward. Surrogate models
8 trained to simulate the behavior of structural fire engineering (SFE) models predict the response
9 at negligible computational expense, thereby allowing for rapid probabilistic analyses and
10 design iterations. Herein, a framework is proposed for the probabilistic analysis of fire exposed
11 structures leveraging surrogate modeling. As a proof-of-concept a simple (analytical) non-
12 linear model for the capacity of a concrete slab and an advanced (numerical) model for the
13 capacity of a concrete column are considered. First, the procedure for training surrogate models
14 is elaborated. Subsequently, the surrogate models are developed, followed by a probabilistic
15 analysis to evaluate the probability density functions for the capacity. The results show that
16 fragility curves developed based on the surrogate model agree with those obtained through
17 direct sampling of the computationally expensive model, with the 10^{-2} capacity quantile
18 predicted with an error of less than 5%. Moreover, the computational cost for the probabilistic
19 studies is significantly reduced by the adoption of surrogate models.

20 **Keywords:** Structural fire safety, Probabilistic studies, Regression, Surrogate modeling,
21 Reinforced concrete.

22

23 **1 Introduction**

24 The fire safety design of structures is traditionally done through the application of prescriptive
25 guidance and code-based recommendations, to meet prescribed nominal fire resistance
26 requirements (ISO, 2019). The fire resistance requirements themselves, as well as the
27 considered nominal fire exposures, load combinations, characteristic material properties, safety
28 factors and limit criteria, all contribute to attaining an adequate level of safety in case the as-
29 built structure experiences a (real) fire. The obtained safety level when applying the traditional
30 design procedure is, however, unknown, and the attainment of an adequate safety level is
31 fundamentally based on precedent (Van Coile et al., 2019). The above implies that the updating
32 of traditional design approaches to adjust to innovations in the built environment or to specify
33 requirements for exceptional designs (Hopkin et al., 2017) relies on ‘lessons learned from
34 failure’ (Spinardi et al., 2017). However to avoid disaster, to allow for the safe introduction of
35 design innovation and the specification of adequate provisions for exceptional structures, and
36 to properly mitigate evolving risk exposure (for example due to climate change and
37 urbanization (McNamee et al., 2019), an explicit consideration of the risk profile of the structure
38 is necessary (Van Coile et al., 2019). In other words, the full range of possible fires, and their
39 associated probabilities must be taken into account, as well as the uncertainties in the structural
40 fire performance and resulting consequences. The current paper is concerned specifically with
41 the efficient probabilistic evaluation of structural fire performance.

42 The probabilistic structural fire analysis can, in principle, be done through repeated evaluation
43 of the structural model for different realizations of the stochastic variables. Such a “Monte
44 Carlo” approach has been applied for example by Heidari et al. (2019) and Van Coile et al.
45 (2014) for a fire-exposed concrete slab, and by Guo et al. (2013), Elhami Khorasani et al. (2015)
46 and Hopkin et al. (2018) for an insulated steel member. A drawback of the Monte Carlo
47 approach is the computational expense implied by the repeated sampling. More efficient

48 stochastic modelling procedures have been applied to structural fire engineering (SFE), for
49 example by Gernay et al. (2019a) and Guo et al. (2015). While both studies managed to reduce
50 the number of simulations drastically, both require additional expert knowledge and careful
51 error analysis. Furthermore, these efficient methodologies still do not allow for quasi-
52 instantaneously updating the probabilistic structural fire analysis during design iterations. This
53 limitation is especially relevant where the structural fire analysis involves a large and complex
54 structural model.

55 The preceding paragraphs indicate a need for a probabilistic structural fire analysis
56 methodology which is (i) conceptually easy to understand; and (ii) allows for fast design
57 iterations. One promising approach is the use of fragility curves. Commonly used to represent
58 the exceedance probability of a predefined damage state in function of an intensity measure or
59 engineering demand parameter, fragility curves have been derived for SFE, for example, by
60 Gernay et al. (2016, 2019b) for steel frame buildings through Monte Carlo approaches, and by
61 Ioannou et al. (2017) for reinforced concrete buildings through expert elicitation. If reference
62 fragility curves are listed (i.e. are precalculated), or can be efficiently evaluated, then the
63 probabilistic approach can find application in design practice. Such an approach is well-
64 developed in earthquake engineering and multiple SFE studies, such as Hamilton (2011), Lange
65 et al. (2014) and Shrivastava et al. (2019), have focused on applying these earthquake
66 procedures to structural fire design. In earthquake engineering, the computational expense is
67 commonly limited by assuming a lognormal distribution for the fragility curve, see e.g. (Baker
68 and Cornell, 2006). Such an assumption may allow for a more efficient evaluation, but can
69 however be inappropriate for SFE, as illustrated in (Gernay et al., 2019b) and (Van Coile et al.,
70 2013). Furthermore, reducing the number of computationally expensive model evaluations is
71 helpful, but does not resolve the fundamental issue that considerable effort and expert handling
72 is required when running computationally advanced models. The option of pre-calculated

73 fragility curves being listed by industry organizations, academic institutions or standardization
74 bodies (as is done for seismic design, see FEMA P58) has been advocated for SFE in (Van
75 Coile et al., 2020), but is difficult to achieve without further simplification or intermediate steps,
76 considering the infinite number of design alternatives, even when considering isolated
77 members.

78 In summary, for probabilistic approaches to find application in SFE design, a computationally
79 efficient methodology which does not rely on the direct use of advanced numerical models to
80 evaluate design iterations is advantageous. Taking into account recent applications of Machine
81 Learning (ML) techniques for fire safety applications, e.g. Dexters et al. (2019), Naser (2019a),
82 and Fu (2020), the hypothesis is put forward here that ML approaches can be instrumental in
83 achieving the above computationally efficient methodology. More specifically, if the advanced
84 numerical models currently used in SFE can be accurately approximated by a surrogate model
85 developed through ML, then probabilistic studies for a fire exposed structure can be achieved
86 quasi-instantaneously with limited loss of accuracy. Furthermore, fast design iteration can then
87 be achieved at negligible additional computational cost.

88 The study presented further acts as a proof-of-concept for probabilistic SFE evaluations
89 supported by surrogate modelling. The structure of the paper is as follows. Section 2 starts with
90 a succinct state-of-the-art discussion on ML techniques in SFE. It is concluded that regression-
91 based surrogate modelling will be explored further in this study, being both intuitive and
92 straightforward in its implementation. Section 2 then continues with a description of the
93 procedures for training a regression-based surrogate model. Subsequently, Section 3
94 demonstrates the development and effectiveness of a surrogate model for (i) a computationally
95 less demanding test case of a concrete slab with known temperature profile; and (ii) a concrete
96 column taking into account geometric imperfections. Finally, in Section 4 fragility curves
97 (cumulative density functions) are evaluated for the test cases, using both the original (“actual”)

98 model and the surrogate model. The comparison between the obtained distributions validates
99 the proof-of-concept for probabilistic analysis of fire exposed structures through regression-
100 based surrogate models.

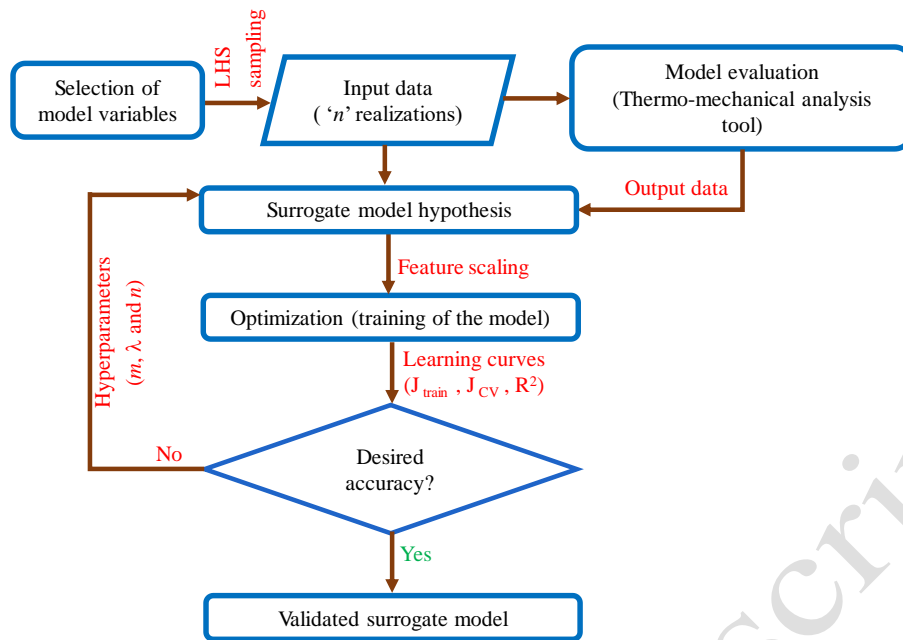
101

102 **2 Regression-based surrogate modelling**

103 Surrogate models derived through ML techniques have been used to evaluate the response of
104 physical systems in a wide range of fields (Forrester et al., 2008; James et al., 2013). The applied
105 techniques include regression, genetic algorithm, and artificial neural networks (ANN). These
106 approaches, when properly used (within the boundaries of the physical system, maintaining
107 interpretability and avoiding the black box effect for the trained model (Rudin, 2019)), provide
108 useful and efficient tools for engineers. While application of ML approaches in fire safety
109 engineering is relatively new, an increasing number of studies have been published in recent
110 years. Dexters et al. (2019), for example, applied regularized logistic (lasso) regression for the
111 prediction of flashover in a scaled fire compartment with sandwich panel walls. Their trained
112 model was presented as a dynamic tool for specifying new test configurations. In the area of
113 structural fire engineering (SFE), a series of studies have been initiated by Naser. In (Seitllari
114 and Naser, 2019) for example, multi-linear regression, genetic algorithm and ANN were
115 adopted to predict explosive spalling phenomena for a fire exposed concrete column. The
116 genetic algorithm was reported to achieve a spalling prediction accuracy of about 95 %. Naser
117 further explored ML methodologies for the prediction of the fire resistance of timber elements
118 and bridge vulnerabilities (Naser, 2019a; Naser, 2019b). Other recent applications of ML in the
119 field of SFE can be found for example in (Fu, 2020) and (Panev et al., 2021). This recent
120 literature suggest a wide application range for ML techniques in fire safety engineering, hardly
121 explored.

122 Regression is arguably better suited to construct interpretable surrogate models than other ML
123 techniques such as ANN, especially when considering simple relationships such as polynomial
124 functions, because the regression coefficients directly inform about the contribution of the
125 respective parameters (features) in the considered model output. These features relate to the
126 selected physical parameters, such as the concrete cover or fire load density, which are
127 considered to govern the model output of interest, such as the fire resistance or the occurrence
128 of flashover in a compartment. Considering the above, polynomial regression-based surrogate
129 modeling is adopted here to approximate the response of fire exposed structural elements.

130 Figure 1 shows the steps for the development of a regression-based surrogate model. These
131 steps are discussed in detail in the following paragraphs. Firstly, the basic input variables must
132 be selected, and a sampling scheme applied to obtain the corresponding model realizations
133 (Section 2.1). Then, a (polynomial) regression function is specified which acts as a hypothesis
134 for the surrogate modelling (Section 2.2). This surrogate model hypothesis defines the model
135 ‘features’, whose relationship determines the response of a physical system. Finally, the
136 regression coefficients are determined through an optimization procedure, such as gradient
137 descent, during which a ‘cost function’ is minimized (Section 2.3). The optimization however
138 highlights a number of issues related to the varying magnitude and dimensionality of the
139 features. To avoid these, the features are scaled (2.4). Furthermore, issues of overfitting and
140 underfitting of the model may occur (2.5). Finally, the accuracy of the trained model must be
141 determined, and the applied model (hyper-)parameters, such as the number of sampling points,
142 must be confirmed, which is done through application of the cross-validation and test data (2.6).



143

144

Figure 1 Methodology for regression based surrogate modeling

145

2.1 Selection of model variables, input data generation, and model evaluation

146

The first step involved in the development of a surrogate model through polynomial regression is the selection of the model variables, on which the behavior of the computationally expensive physical system depends. If $\mathbf{x}=[x_1, x_2, x_3, \dots, x_{r-1}, x_r]$ represent a vector of variables, then the response, y of the physical system, $h(\mathbf{x})$ is given by:

150

$$y = h(\mathbf{x}) \quad (1)$$

151

The surrogate model is generally developed for a specific purpose. It is thus not necessary to consider all possible parameters of the physical system as input variables for developing a surrogate model. This implies that parameters which are considered fixed within the scope of the model are not considered explicitly for the surrogate model development. Therefore, in the current study only the (independent) variables that are considered uncertain in the probabilistic assessment are considered as input variables for the surrogate model.

157

Once the model variables are chosen, an appropriate sampling scheme needs to be adopted to evaluate the model realizations, y_i , to train a surrogate model. These realizations are obtained

158

159 with a sophisticated model of the physical system (e.g. a finite element model). The sampling
160 scheme should cover the entire parameter space of interest, while at the same time limiting the
161 number of realizations as much as possible (Forrester et al., 2008). A Latin Hypercube
162 Sampling (LHS) scheme will be adopted in the current study for the input data (Olsson et al.,
163 2003). Importantly, modeling limitations of the finite element model will also apply to the
164 surrogate model. If the finite element model is unable to capture shear failure, then the same
165 limitation will apply to the surrogate model.

166 2.2 Surrogate model hypothesis

167 For polynomial regression, the hypothesis for the surrogate model is a summation of polynomial
168 terms. A 2nd order polynomial hypothesis ($m = 2$) for the surrogate model, considering two
169 independent variables x_1 and x_2 can be given by Eq.(2). Here $\hat{y} = \hat{h}(\mathbf{x})$ indicates the surrogate
170 model approximation for the actual (physical) model $y = h(\mathbf{x})$, $[\theta_0, \theta_1, \dots, \theta_5]$ are regression
171 coefficients, in which θ_0 refers to the bias term, x_1 and x_2 are the realizations of the independent
172 variables, x_1^2 and x_2^2 are higher order terms, and x_1x_2 is the interaction term of the surrogate
173 model. Together, the first order, higher order and interaction terms are the ‘features’ for the
174 regression surrogate model. For further discussion on the regression hypothesis reference is
175 made to (Forrester et al., 2008).

$$176 \quad \hat{y} = \hat{h}(\mathbf{x}) = \theta_0 + \theta_1x_1 + \theta_2x_2 + \theta_3x_1^2 + \theta_4x_2^2 + \theta_5x_1x_2 \quad (2)$$

177 2.3 Cost function and model fitting

178 The regression coefficients θ in Eq. (2) are estimated through the minimization of the cost
179 function, ‘ $J(\theta)$ ’, which is a measure of error in prediction for a given data. The cost function for
180 training a surrogate model (James et al., 2013) is given by Eq. (3) and can be understood as the
181 half the mean squared error of the prediction for the training data set.

182
$$J(\theta) = \frac{1}{2n} \sum_{i=1}^n (\hat{h}(x_i) - y_i)^2 \quad (3)$$

183 An optimization algorithm needs to be adopted for the determination of the coefficients θ_0 ,
184 $\theta_1, \dots, \theta_r$, which minimize the cost function in Eq.(3). In this regard, numerous optimization
185 algorithm for cost function optimization can be found for example in the Python Scipy library
186 (Virtanen et al., 2020). In the current study, the gradient descent algorithm is selected (Forrester
187 et al., 2008; Du et al., 2018). The gradient descent algorithm follows a downhill approach for
188 the minimization of the cost function, whereby regression coefficients are updated at each
189 iteration in the opposite direction to the positive gradient of $J(\theta)$. The regression coefficients
190 for the surrogate model adopted at each subsequent iteration are given by:

191
$$\theta_l = \theta_l - \alpha \frac{\partial}{\partial \theta_l} J(\theta) \quad (4)$$

192 where, α is the learning rate of the surrogate model for gradient descent method. The iteration
193 is done simultaneously for all coefficients l . Convergence is achieved once the difference in
194 cost function evaluation between iterations falls below a predefined tolerance. The estimated
195 regression coefficients can then be used to predict the response of the physical system.

196 **2.4 Feature scaling**

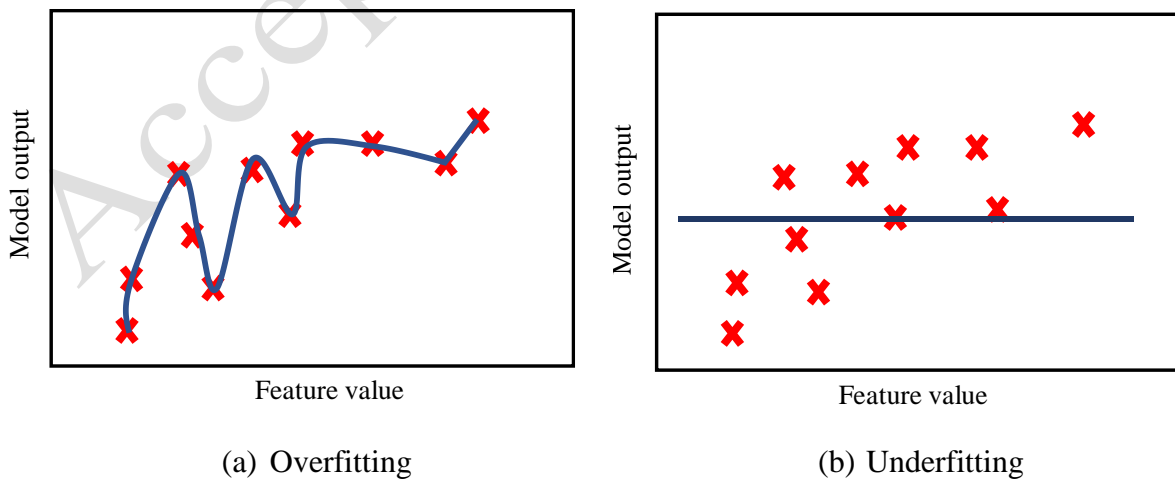
197 The procedure outlined above with the cost function of Eq. (3) has as disadvantage that the cost
198 evaluation is dependent on the dimension of the model output. This makes it difficult to
199 recommend a tolerance factor denoting convergence, and results in an unequal weighting of
200 features in the coefficient updating of Eq. (4). Consequently, the features need to be scaled so
201 that all variables are of comparable dimensions in order to implement regression algorithms.
202 Here, a standardization technique is implemented which normalizes the independent variables,
203 i.e. the features are scaled to have zero mean and unit variance. The normalized independent

204 variables are given by Eq. (5), with c the original feature value, μ_c the feature mean, σ_c the
205 feature standard deviation, and c_{norm} the normalized feature value.

206
$$c_{norm} = \frac{c - \mu_c}{\sigma_c} \quad (5)$$

207 **2.5 Fitting issues**

208 The predicted response for the surrogate model depends on how well it was trained, which
209 relates to the adopted order of polynomial (m) and size of the sample (n). An inappropriate
210 order of polynomial for the surrogate model might lead to underfitting or overfitting of the
211 training data (Forrester et al., 2008). Although an overfitted surrogate model can accurately
212 predict the response for training data, it might be incapable of predicting the results for unseen
213 cases. In contrary, an underfitted surrogate model predicts the results for both the trained and
214 untrained data inaccurately. Figure 2 illustrates these concepts. Likewise, if the size of the
215 sample is not sufficient to map the entire sample space of the variables, the surrogate model
216 might be incapable of predicting the response of the physical system precisely. Thus, an
217 appropriate size of the LHS sample needs to be determined for training a surrogate model to
218 predict the response accurately.



219 Figure 2 Issues in developing surrogate model

220 The issue of overfitting of the training data can be addressed by introducing a regularization
221 parameter (λ) in the cost function. Eq. (6) gives an expression for a regularized cost function to
222 train a surrogate model.

$$223 \quad J_{\text{learn}}(\theta) = \frac{1}{2n} \sum_{i=1}^n (\hat{h}(\mathbf{x}_i) - y_i)^2 + \frac{\lambda}{2n} \sum_{l=1}^r \theta_l^2 \quad (6)$$

224 The regularization parameter penalizes the coefficients in the surrogate model. This means that,
225 if higher order polynomials are adopted with more non-zero coefficients, the cost function is
226 artificially increased by an additional cost term. As the value of the regularization parameter
227 influences the result of the optimization, it needs to be chosen wisely. The same statement
228 applies to the order of the polynomial model and the number of training samples. These
229 parameters are known as hyperparameters and they can be determined through application of
230 learning curves.

231 **2.6 Hyperparameters, learning curves and performance evaluation**

232 To evaluate and improve the performance of the machine learning algorithms (i.e. perform
233 hyperparameter optimization), three different input data sets are considered: a training set, a
234 cross-validation set and test data set. The training set is applied to find the optimum vector of
235 coefficients, θ , for given hyperparameters, while the cross-validation data set is used to
236 evaluate the optimum value of the hyperparameters, i.e. to distinguish between the different
237 models trained on the training set. Finally, the test data set allows to evaluate the prediction
238 accuracy of the surrogate model on an unseen set of datapoints.

239 A complete LHS sample is considered as a training set to ensure that the entire sample space of
240 independent variables is assessed by the computationally expensive physical system. The cross-
241 validation and test data set can however be generated randomly (Monte Carlo simulation). The
242 prediction errors for the training (J_{train}) and cross-validation data sets (J_{cv}), are given by:

243
$$J_{\text{train}}(\theta) = \frac{1}{2n_{\text{train}}} \sum_{i=1}^{n_{\text{train}}} \left(\hat{h}(\mathbf{x}_{\text{train},i}) - y_{\text{train},i} \right)^2 \quad (7)$$

244
$$J_{\text{cv}}(\theta) = \frac{1}{2n_{\text{cv}}} \sum_{i=1}^{n_{\text{cv}}} \left(\hat{h}(\mathbf{x}_{\text{cv},i}) - y_{\text{cv},i} \right)^2 \quad (8)$$

245 Learning curves refer to the plot of these estimated training and cross-validation costs, where a
 246 hyperparameter to be optimized is varied, while other parameters are assumed constant. The
 247 hyperparameters in the current study are the regularization parameter value (λ), the order of the
 248 polynomial model (m), and the size of the LHS sample (n). The optimum hyperparameters are
 249 determined as those for which the cross-validation cost function indicates that further
 250 complexity does not result in a significant reduction in cross-validation cost (estimation error),
 251 or even results in a cost increase.

252 After the evaluation of the hyperparameters, the performance of the developed surrogate model
 253 can be assessed based on test data set, for which the coefficient of determination, R^2 (Draper
 254 and Smith, 1998) can be determined. The R^2 value refers to the prediction efficiency of the
 255 model and is given by:

256
$$R^2 = 1 - R_{\text{res}} / R_{\text{tot}} \quad (9)$$

257 where, $R_{\text{res}} = \sum_{i=1}^{n_{\text{test}}} \left(\hat{h}(\mathbf{x}_{\text{test},i}) - y_{\text{test},i} \right)^2$ and $R_{\text{tot}} = \sum_{i=1}^{n_{\text{test}}} \left(y_{\text{test},i} - \bar{y}_{\text{test}} \right)^2$ are the residual and total sum of
 258 squares, respectively, in which \bar{y}_{test} is the mean of the test data set. The value of the coefficient
 259 of determination ranges from 0 to 1, with '1' representing a perfectly fitted surrogate model.

260

261 3 APPLICATION: SURROGATE MODEL DEVELOPMENT

262 To demonstrate the application of regression-based surrogate models to SFE, a simple and an
263 advanced non-linear model are considered as physical systems in this study. The terms ‘actual
264 models’ and ‘physical systems’ are further used interchangeably. In the above “simple” refers
265 to an SFE model which does not require numerical approaches. The considered simple model
266 is presented in Section 3.1 and relates to the bending moment capacity of a simply supported
267 concrete slab, considering known temperature for the reinforcement. The advanced model on
268 the other hand involves significant computational cost. The considered advanced non-linear
269 models is presented in Section 3.2 and relates to the load bearing capacity of a concrete column
270 under fire considering second order effect.

271 3.1 Simple non-linear model: concrete slab bending capacity for known rebar 272 temperature

273 3.1.1 Physical system: analytical equation for moment capacity of RC slab

274 The analytical model adopted by Van Coile et al. (2013) to estimate the resisting moment of a
275 fire exposed RC slab for a known rebar temperature is considered here as a simple non-linear
276 model. The governing equation is given by Eq. (12) where, A_s is the area of tensile reinforcing
277 bars in the slab, ϕ is the diameter of the tensile reinforcing bars in the slab, h and b refer to the
278 depth and width of the slab, c is the concrete cover to the reinforcement, $f_{c,20^\circ\text{C}}$ refers to the
279 20°C compressive strength of the concrete, and $f_{y,20^\circ\text{C}}$ and $k_{fy(T)}$ are respectively the
280 reinforcement yield strength at 20°C and the yield strength retention factor at T degrees Celsius.

$$281 \quad M_R = A_s k_{fy(T)} f_{y,20^\circ\text{C}} \left(h - c - \frac{\phi}{2} \right) - 0.5 \frac{(A_s k_{fy(T)} f_{y,20^\circ\text{C}})^2}{b f_{c,20^\circ\text{C}}} \quad (12)$$

282 The RC slab is considered to be exposed to the fire at the bottom face, and to have sufficient
 283 depth for the concrete compressive zone to retain its strength (i.e. remain below approximately
 284 200°C).

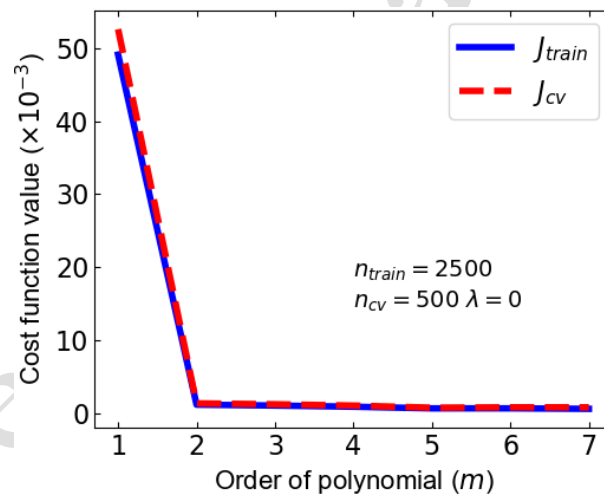
285 3.1.2 Development of the surrogate model

286 To develop the surrogate model following the procedure of Figure 1, first the model
 287 variables based on Eq. (12) are identified as $f_{c,20^{\circ}\text{C}}$, $f_{y,T} = (k_{fy(T)} \cdot f_{y,20^{\circ}\text{C}})$, c , h and A_s . The slab
 288 capacity is evaluated for a fixed unit width ($b=1\text{m}$) and the reinforcing bars are considered to
 289 be 12 mm in diameter. Next, the range of interest for the surrogate model is specified for each
 290 of the independent variables by an upper and a lower limit, as listed in Table 1. The surrogate
 291 model is intended to accurately simulate the physical system within these bounds for the
 292 variables, and therefore a uniform distribution is adopted, ensuring equal weighting in the
 293 subsequent sampling. Adopting the LHS scheme, the required input data are generated, as
 294 discussed in Section 2.1, for the cross-validation set a Monte Carlo scheme is applied. With Eq.
 295 (12) representing the physical system, the bending moment of the slab (the ‘model evaluation’
 296 or output) can easily be evaluated for the considered combinations of input variables. The
 297 combinations of input variables and the corresponding bending moment capacities are then used
 298 to develop the surrogate model.

299 Table 1: Model variables for the fire exposed RC slab case study, with their lower and upper
 300 limits for the sampling space and dimensions

Independent variables	Lower limit	Upper limit	Unit	Distribution
Concrete strength, $f_{c,20^{\circ}\text{C}}$	15	80	MPa	
Rebar strength, $f_{y,T}$	100	1000	MPa	
Concrete cover, c	20	70	mm	Uniform
Slab thickness, h	100	300	mm	
Reinforcement area, A_s	0.10	0.25	% (section area)	

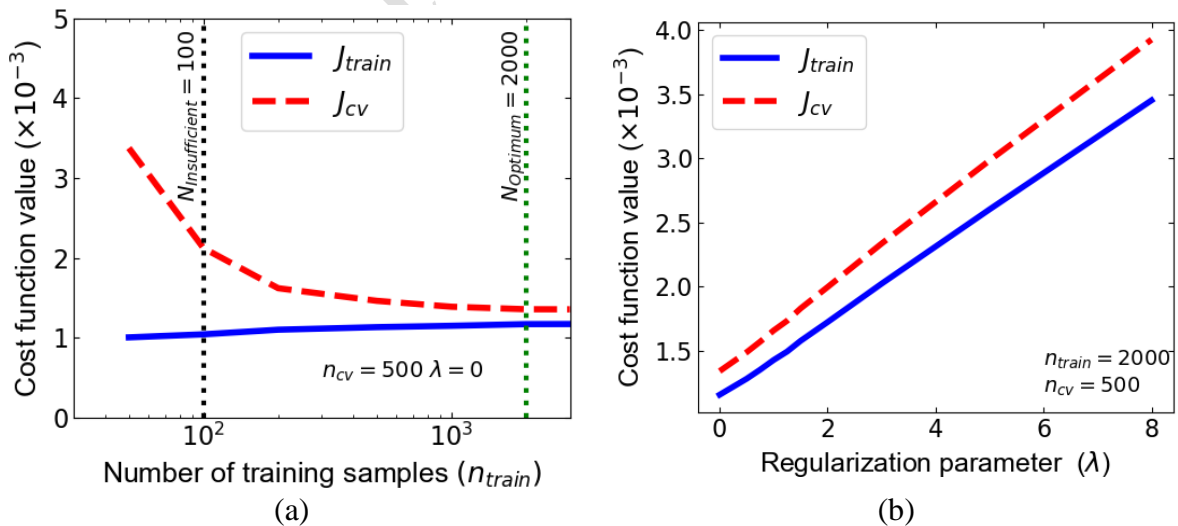
301 As discussed in Section 2.6, the surrogate model is dependent on the considered
 302 hyperparameters (number of training samples n , regularization parameter λ , order of the model
 303 m). The optimum values for the hyperparameters are estimated based on the cost functions (J_{train}
 304 and J_{cv}), i.e. by establishing learning curves. Figures 3 and 4 show the developed learning
 305 curves for the surrogate model to determine the hyperparameters in the test case. According to
 306 Figure 3, the 2nd order polynomial approximation has higher accuracy than the 1st order
 307 polynomial. However, there is no significant improvement for surrogate models with order
 308 ' m ' > 2. The computational burden also gradually increases with the adoption of a higher order
 309 hypothesis for the surrogate model, due to the increased number of features with higher order
 310 polynomials and interaction terms, complicating the optimization. Therefore, a 2nd degree
 311 polynomial is adopted as surrogate model hypothesis for the fire exposed RC slab.



312 Figure 3 Cost function value for the surrogate model, in function of the order m of the
 313 regression model hypothesis
 314

315 Figure 4 helps determining the hyperparameters (n and λ) for the considered surrogate model.
 316 Based on Figure 4(a), an optimum size of the LHS sample for training the surrogate model can
 317 be evaluated. In the figure, mean values for J_{train} and J_{cv} are plotted against the training sample
 318 size for a 2nd order surrogate model, considering a constant cross-validation set n_{cv} of size 500.
 319 Mean values are listed because for low sample sizes, the cost evaluation can depend on the

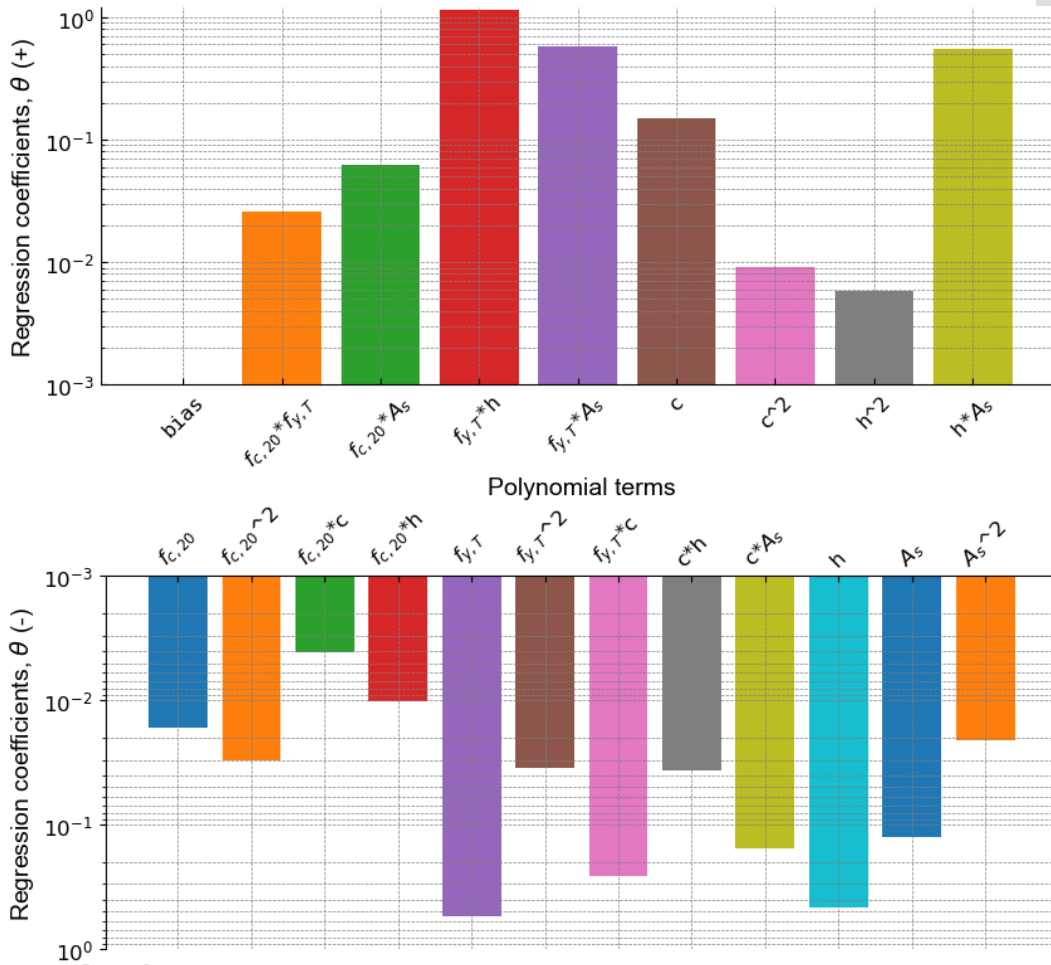
320 specific set of LHS realizations. Therefore, a repeated sampling approach is adopted, where 10^3
 321 LHS samples for each of the training sets are developed. As the J_{train} and J_{cv} have converged
 322 for a training set of 2000 LHS samples, this sample size is observed to be sufficient (i.e. optimal)
 323 for the surrogate model. On the other hand, based on the learning curves 100 LHS sample points
 324 is insufficient for developing a precise surrogate model, as a further increase of n results in a
 325 significant decrease of J_{cv} . The regularization parameter has not been considered for the
 326 estimation of both the optimum order of polynomial and number of training sample size. For
 327 the considered surrogate model order and number of training samples this is reasonable, as
 328 demonstrated in Figure 4(b) where J_{train} and J_{cv} are plotted in function of the regularization
 329 parameter λ . The regularization parameter is found to have no influence over the developed
 330 surrogate model and thus can be neglected for the development of the surrogate model here.
 331 However, the regularization parameter becomes important when a larger model order is
 332 considered. These situations however do not result in a lower J_{cv} than for the hyperparameter-
 333 combination ($n_{train} = 2000$, $m = 2$ and $\lambda = 0$), while at the same time increasing computational
 334 cost significantly.



335 Figure 4 Cost function value for the surrogate model, in function of (a) the number of training
 336 samples, n_{train} and (b) the regularization parameter, λ

337 **3.1.3 Evaluation of surrogate model performance and discussion**

338 Figure 5 represents the developed surrogate model based with assessed optimum
 339 hyperparameters ($n_{train} = 2000$, $m = 2$ and $\lambda = 0$). In the Figure, the regression coefficients are
 340 shown for the normalized features of the surrogate model (2nd degree polynomial model). The
 341 values for these coefficients are also listed in the Annex.

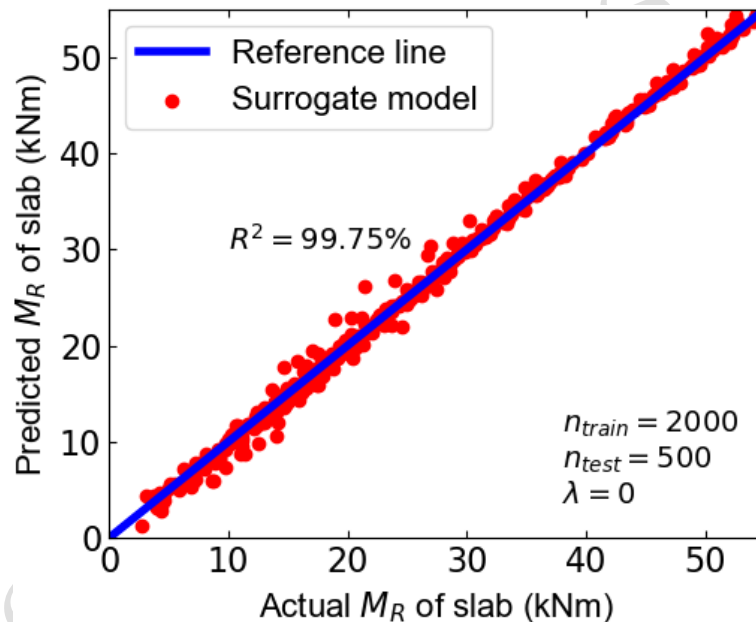


342 Figure 5 Obtained regression coefficients for 2nd order surrogate model with normalized
 343 features. Positive coefficients in the upper graph, negative coefficients in the lower graph.

344 These regression coefficients, also referred to as ‘weights’ of a particular feature, indicate the
 345 influence of respective features on the response of the system. For example, the polynomial
 346 term ‘ $f_{y,T} * h$ ’ has a higher value for its regression coefficient than the other polynomial terms,
 347 and thus has higher influence on the moment capacity of the slab. The surrogate model thus can

348 also be helpful in assessing the influence of a particular variable or combination of variables on
349 the response of the actual model.

350 The performance of the developed surrogate model is evaluated by comparing the actual and
351 predicted response for the test data set (unseen random data), where the coefficient of
352 determination (R^2) is estimated as stated in Section 2.6. Figure 6 shows the comparison of the
353 moment capacity of the RC slab for the 500 realizations of the test set, as evaluated respectively
354 by the actual model and the developed surrogate model. The R^2 value for the surrogate model
355 of RC slab is found to be 99.75 %, indicating very good accuracy.



356

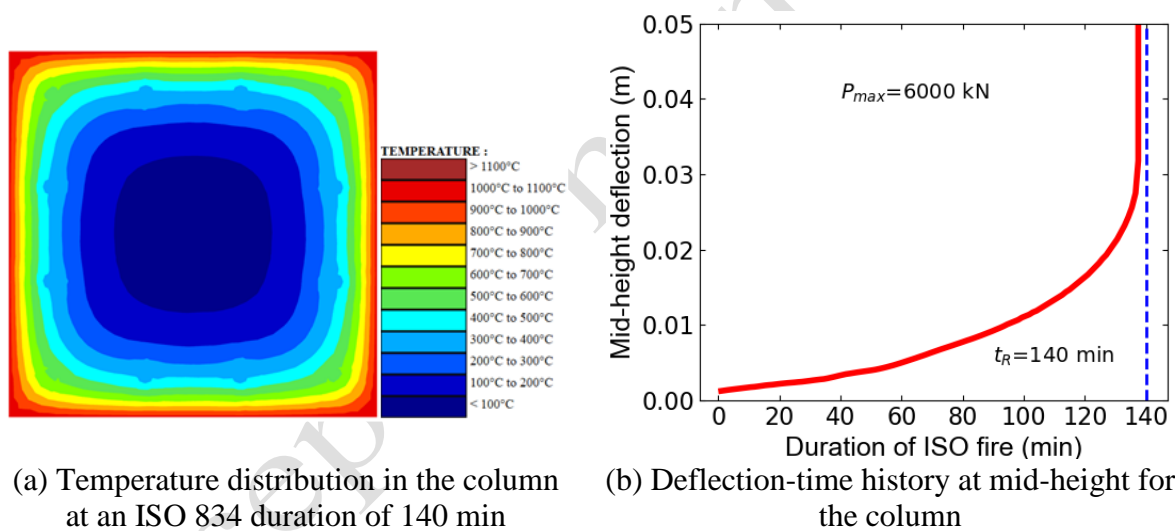
357 Figure 6 Performance of the developed surrogate model for the moment capacity of RC slab
358 with known rebar temperature

359 3.2 Advanced non-linear model: Finite element evaluation of RC column load bearing 360 capacity

361 3.2.1 Physical system

362 This model deals with the axial load bearing capacity of an RC column exposed to the ISO 834
363 standard fire on four sides. A probabilistic study for the considered column has been presented

364 in (Van Coile et al., 2020) and has been incorporated in ISO/TR 24679-8:2020 (ISO, 2020).
 365 The column capacity assessment is done through the dedicated Finite Element (FE) software
 366 SAFIR® (Franssen and Gernay, 2017). The column cross-section is 500 mm × 500 mm with 12
 367 reinforcing bars of 20 mm diameter. The height is 4 m and the column is pinned at the bottom
 368 and has a roller support at the top (Van Coile et al., 2020). The concrete is a C30/37 and the
 369 reinforcing steel is of grade 500. The thermal response is modeled in accordance with Eurocode
 370 EN 1992-1-2:2004. Figure 7 shows the thermal and mechanical response for the above
 371 considered RC column exposed to ISO 834 fire, with an axial load of 6000 kN at an eccentricity
 372 of 1.5 cm. In this specific evaluation, the column is found to have fire resistance of 140 min,
 373 with the temperature of the rebars reaching 598°C.



374 Figure 7 Thermal and mechanical response for RC column exposed to ISO 834 fire, with an
 375 axial load of 6000 kN at an eccentricity of 15 mm

376 3.2.2 Development of the surrogate model

377 Six variables are considered to govern the model response. These are the retention factor
 378 quantile parameters for the concrete compressive strength (ϵ_{kfc}) and reinforcement yield stress
 379 (ϵ_{kfy}), the concrete cover (c), average eccentricity (e), out of straightness (oos), out of plumbness
 380 (oop) and the applied load (P). The parameters ϵ_{kfc} and ϵ_{kfy} are parameters defining the quantile

381 of the retention factors at elevated temperature in accordance with the strength retention models
382 by Qureshi et al. (2020). The model variables e , oos and oop refers to the three basic
383 eccentricities associated with the column, as considered in JCSS probabilistic model code
384 (2013).

385 Next, the input data for the physical model evaluation is obtained through an LHS sample of
386 the model variables. The considered range for the sample space is listed in Table 2. An initial
387 training sample size of 10^4 realizations is considered, while a separate (fixed) Monte Carlo set
388 of 1250 realizations is evaluated as a cross-validation data set.

389 Having evaluated the physical model for the input realizations of the model variables, the
390 surrogate modelling hypothesis is defined. To allow for comparison with the (numerically
391 expensive) evaluations by Van Coile et al. (2020), the surrogate model is developed to predict
392 the maximum load bearing capacity P_{max} of the concrete column, considering a specified ISO
393 834 exposure duration and specific realizations for the other model variables. In other words,
394 the evaluated fire resistance time t_E of the RC column is considered as input parameter for the
395 surrogate model development, while the associated applied load P is to be considered as the
396 response by the surrogate model. To elucidate the motivation for the above procedure further,
397 note that in Van Coile et al. (2020) the maximum load P_{max} for a given ISO 834 standard fire
398 duration t_E was determined through an iterative search algorithm for P_{max} . The corresponding
399 probabilistic analysis was very computationally expensive owing to the need to perform
400 multiple finite element evaluations for each sample realization. The surrogate modelling
401 procedure applied here is intended to result in a computationally much more efficient process.
402 Note that for a given set of parameters, the SAFIR model evaluation is the same irrespective
403 whether this set of parameters was obtained by an iterative approach to find P_{max} for given t_E .

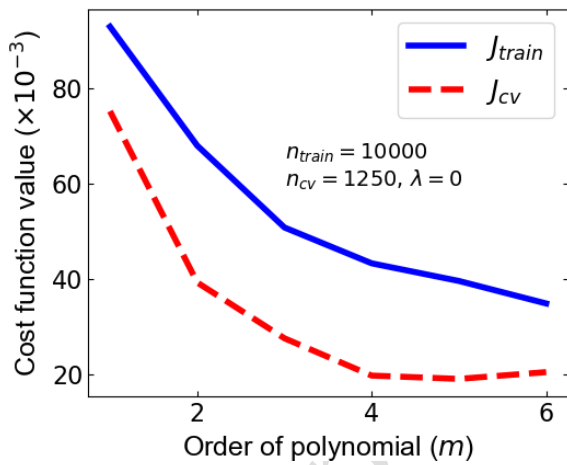
404 It is important to note that the surrogate model aims at approximating the physical system
 405 (SAFIR model) and will thus incorporate the limitations and assumptions of the numerical
 406 model. General assumptions include for example perfect bond between concrete and steel.
 407 Limitations relate for example to the inability of the beam model to consider shear or spalling.
 408 For further overview on the general SAFIR modelling assumptions and limitations, reference
 409 is made to (Franssen and Gernay, 2017). Furthermore, in the current case study, the SAFIR
 410 model takes into account Eurocode material properties. The surrogate model can thus not be
 411 interpreted more generally considering material models from other guidance documents.

412 Table 2. Model variable for the RC column case study, with their lower and upper limits for
 413 the sampling space and dimensions

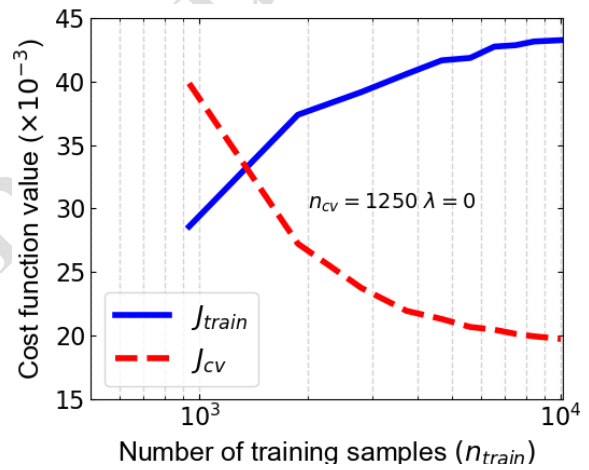
Independent variables	Lower limit	Upper limit	Unit	Distribution
Concrete strength retention factor, ϵ_{kfc}	-4.00	4.00	-	
Rebar yield strength retention factor, ϵ_{kfy}	-4.00	4.00	-	
Concrete cover, c	16	96	mm	Uniform
Average eccentricity, e	-0.03	0.03	mm	
Out of straightness, oos	-0.03	0.03	mm	
Out of plumbness, oop	-0.01	0.01	rad	
Applied load, P	1000	10500	kN	

414 Figure 8 shows the learning curves generated as part of the surrogate model development. Based
 415 on Figure 8(a), a 4th order polynomial is found more precise compared to polynomials with m
 416 ≤ 3 . On the other hand, there is no further significant decrease in error for predictions on the
 417 cross-validation set for $m \geq 5$. Thus, a 4th order polynomial approximation is adopted for the
 418 surrogate model. Similarly, based on Figure 8(b) a training set of 10^4 LHS samples is found
 419 adequate to develop surrogate model since the prediction error on the cross validation set shows
 420 signs of convergence with limited further reduction in J_{cv} for $n_{train} \geq 6000$. In the same way,

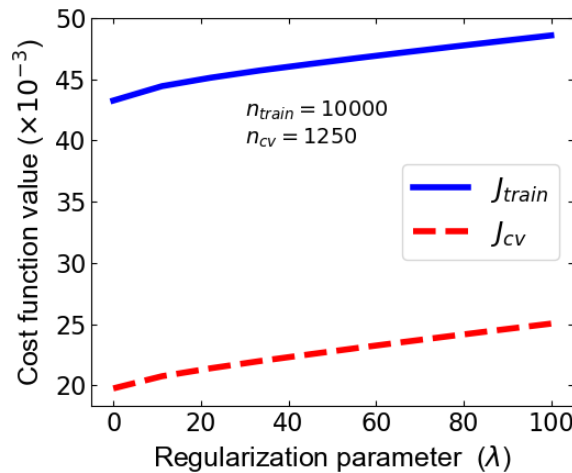
421 Figure 8(c) suggests that the considered surrogate model does not require a regularization
 422 parameter. It can be seen that the learning curves in Figure 8 indicate a higher prediction error
 423 for the training data as compared to the cross validation data. This is however not the case for
 424 $n_{train} = 10^3$, see Figure 8(b). Taking into account this observation, and noting that the LHS
 425 sampling procedure ensures that training samples are generated across the entire space of model
 426 variables, it is hypothesized that the training data sets with a larger number of samples than the
 427 1250 cross validation samples result in a larger probability of obtaining ‘extreme cases’ for
 428 which the model performs less well. This hypothesis will be evaluated in detail as part of follow
 429 up research.



(a)



(b)

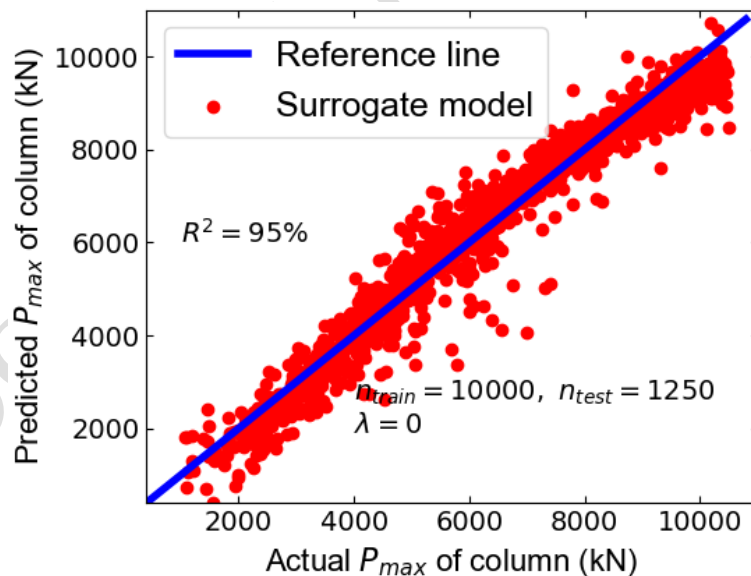


(c)

430 Figure 8 Learning curves to develop surrogate model for RC column under ISO 834 fire

431 3.2.3 Evaluation of surrogate model performance and discussion

432 Figure 9 shows the performance of the developed surrogate model for the test data set. The R^2
433 value for the surrogate model was found to be approximately 95 %. As the considered
434 evaluation of load capacity of column involves complex structural fire calculations, the
435 estimated error can be considered reasonable. Thus, the surrogate model can be considered to
436 effectively simulate the entire thermal and mechanical calculation for FE model of RC column
437 and estimate the load bearing capacity of the RC column for a specified fire duration t_E . It is
438 noteworthy that the evaluation of the test set using the actual SAFIR model took about 60 core-
439 hours on a state-of-the-art PC, while the evaluation of the same test set through the surrogate
440 model is quasi-instantaneous.



441

442 Figure 9 Performance of the developed surrogate model for RC column under ISO 834

443

exposure

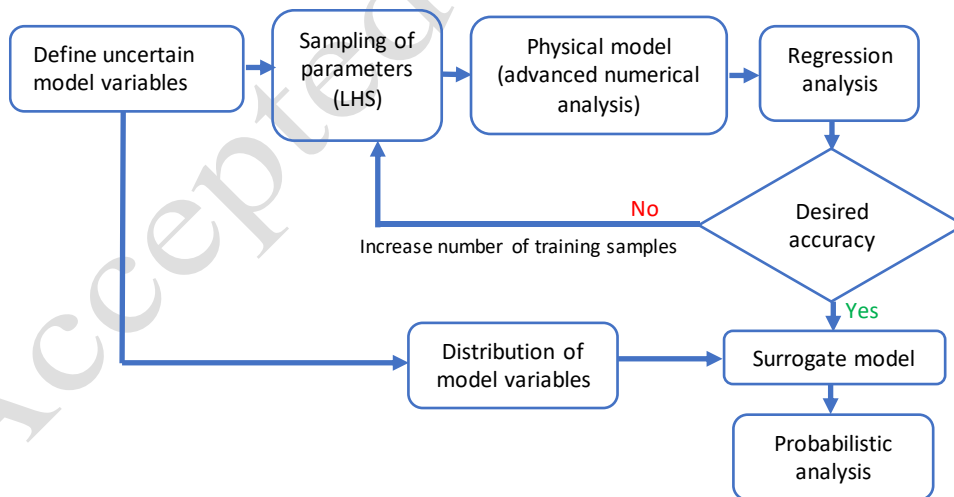
444 As discussed earlier in Section 3.1, the developed surrogate model can be helpful in determining

445 the influencing parameters of the physical system. The duration of fire exposure (t_E) has the

446 highest absolute value for the regression coefficients ($\cong 1.32$) compared to all other polynomial
447 terms and thus can be regarded as the most influencing parameter. The bias term is almost equal
448 to zero and thus has negligible effect on the physical system.

449 4 APPLICATION OF SURROGATE MODELS FOR PROBABILISTIC STUDIES

450 The proposed framework for probabilistic studies of fire exposed structures through regression
451 based surrogate models is visualized in Figure 10. The first steps correspond to the development
452 of the surrogate model as a substitute for the physical system. Once the surrogate model is
453 adequately trained, the probabilistic distributions for the model parameters are considered
454 (based on literature) for the specific design. The probability distribution of the model output is
455 then evaluated by sampling the model variables according to their probabilistic distributions
456 (LHS is adopted herein), and evaluating the surrogate model for each realization. As the
457 surrogate model is not computationally expensive, the probabilistic evaluation can be assessed
458 at limited computational cost.



459

460 Figure 10 Framework for probabilistic studies of fire exposed structures through surrogate
461 modeling approach

462 The framework of Figure 10 is applied to probabilistic studies of the cases of Section 3. The
463 obtained probability density functions (PDF) and cumulative density functions (CDF) are

464 validated against the traditional direct Monte Carlo evaluations of the numerical models (i.e.
465 repeated sampling of the computationally expensive physical system). This is intended to
466 demonstrate the feasibility of the proof-of-concept. Finally, the surrogate models will be
467 employed for probabilistic studies for structural fire scenarios for which no computationally
468 expensive validation is available, demonstrating the practical value of the proposed approach.
469 The proposed approach however comprises

470 **4.1 Simple non-linear model: probabilistic study of a concrete slab bending capacity for** 471 **known rebar temperature**

472 The surrogate model developed in Section 3.1 for the estimation of the moment capacity of an
473 RC slab with known rebar temperature is applied. The temperature distribution in the slab is
474 deterministic, and is evaluated taking into account the recommendations of EN 1992-1-2:2004,
475 using the thermal model as presented by Thienpont et al. (2019). Table 3 shows the probability
476 distribution of the variables, based on Thienpont et al. (2019). The steel yield strength retention
477 factor is multiplied with the mean 20°C yield strength of 581 MPa. In this Table, μ denotes the
478 mean value and σ denotes the standard deviation. To develop the fragility curves, an LHS
479 scheme with 10^4 realizations is adopted.

480 **4.1.1 Nominal ISO 834 exposure**

481 A nominal exposure of 120 min ISO 834 at the bottom face is considered, with convection
482 cooling applied at the top face. Figure 11(a) shows the comparison of the obtained probability
483 density function (PDF) for the actual and surrogate model. The PDF obtained through the
484 surrogate model ($N_{\text{train}} = 2000$) almost coincides with the one obtained through a direct
485 evaluation of the actual model of Eq. (12). The PDF obtained from a surrogate model trained
486 with 100 LHS samples ($N_{\text{insufficient}}$) also agrees, but with a slightly larger difference. The mean
487 value for the bending moment capacity at 120 minutes of ISO 834 exposure is 32.61 kNm
488 according to the actual model, whereas the surrogate models trained with 100 and 2000 LHS

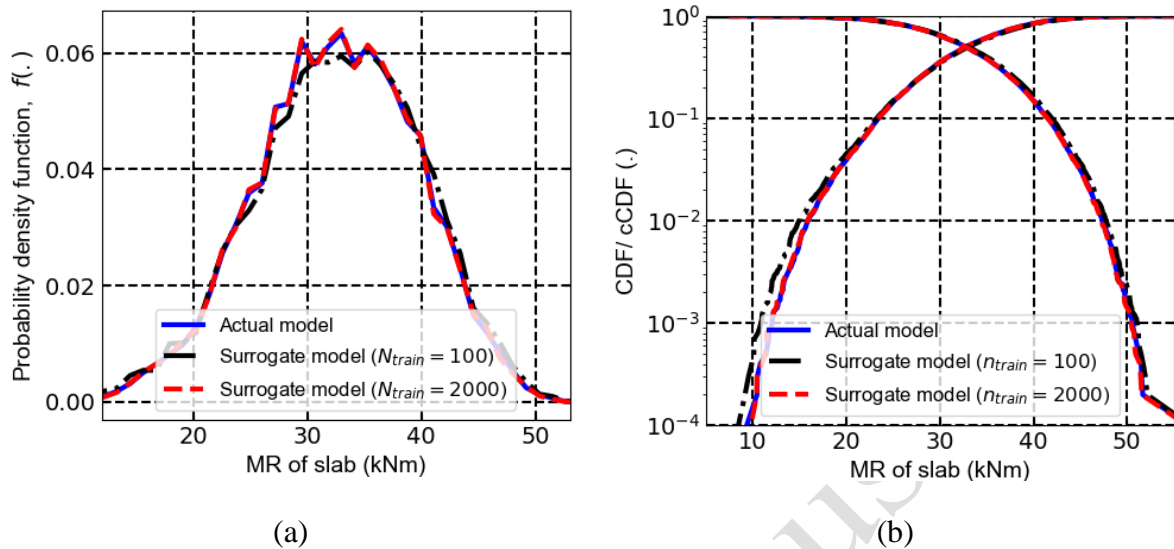
489 samples result in mean value estimates of 32.77 kNm and 32.58 kNm, deviating by 0.5 % and
 490 0.09 % respectively from the actual model's result.

491 Table 3 Probabilistic distributions for the model variables for the RC slab, known rebar
 492 temperature

Stochastic variables	Distribution	Mean	COV
Concrete strength, $f_{c,20^{\circ}\text{C}}$ ($f_{ck,20} = 30$ MPa)	Lognormal	42.9 MPa	0.15
Retention factor for yield strength of rebars, k_{fy}	Logistic model (Qureshi et al., 2020)	Temperature-dependent	Temperature-dependent
Concrete cover, c	Beta [$\mu-3\sigma$; $\mu+3\sigma$]	35 mm	0.14 $\sigma = 5$ mm
Slab depth, h	Normal	200 mm	0.025 $\sigma = 5$ mm
Area of tensile reinforcement, A_s (nominal area $A_{s,nom} = 0.1965$ % of section area)	Normal	$1.02 A_{s,nom}$	0.02

493 Likewise, Figure 11(b) compares the obtained cumulative density functions. Here, the
 494 difference for the surrogate model with $n_{train} = 100$ is more noticeable, notably for the lower
 495 quantiles of the CDF. In Figure 11(b), the 10^{-2} capacity quantile (99 % probability of a larger
 496 capacity) for the RC slab is predicted as 14.91 kNm and 15.83 kNm based on the surrogate
 497 model developed from 100 and 2000 LHS sample, which is very close to the 15.89 kNm
 498 obtained through the actual model. Table 4 lists and compares the actual and predicted moment
 499 capacity of the heated RC slab for different capacity quantiles. The Table shows that even the
 500 10^{-4} quantile capacity of the slab is predicted with great accuracy by the surrogate model.
 501 Therefore, the direct CDF evaluation through 10^4 evaluations of the actual (physical) model
 502 can be accurately approximated by evaluations applying a surrogate model which has been
 503 trained using just 2000 (physical) model evaluations. Although the computational expense is

504 negligible for the considered case, the number of physical model evaluations is reduced
 505 significantly by adopting the surrogate modeling methodology.



506 Figure 11 Comparison of (a) probability density function (PDF) and (b) cumulative density
 507 function (CDF) for the RC slab exposed to 120 min of ISO 834 fire

508 Table 4 Capacity quantiles for the RC slab exposed to ISO 834 fire

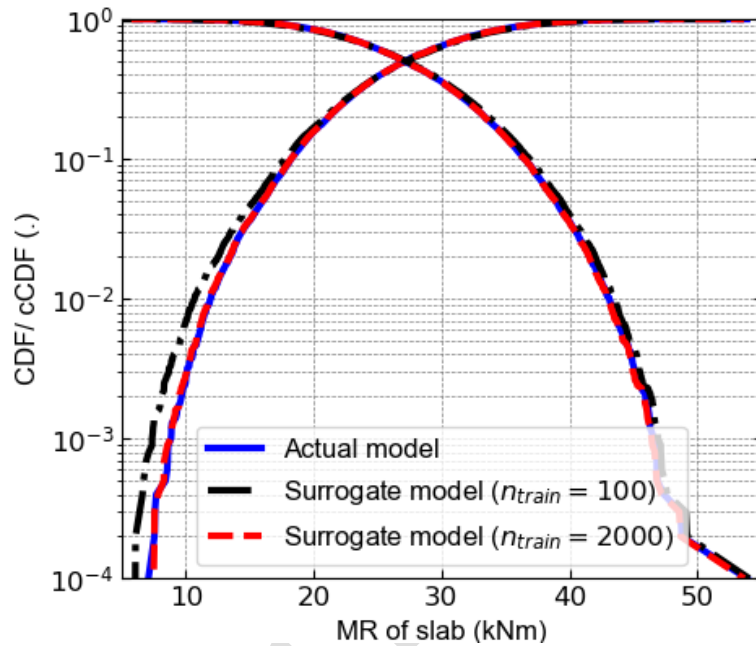
S.N	CDF (.)	M_R of slab (kNm) for ISO fire		
		$n_{train}=100$	$n_{train}=2000$	<i>Actual model</i>
1.	10^{-1}	23.21	23.39	23.40
2.	10^{-2}	14.91	15.83	15.89
3.	10^{-3}	10.86	12.08	12.04
4.	10^{-4}	8.45	9.45	9.34

509 4.1.2 Parametric fire exposure

510 The surrogate models can be applied directly for different fire exposure scenarios. Here, a
 511 Eurocode parametric fire (EN 1991-1-2:2002) with $\Gamma = 1$ and $t_{max} = 120$ min is considered. The
 512 temperature of the reinforcing steel bar is estimated considering a regression model proposed
 513 by Thienpont et al.(2019), which gives the reinforcement temperature for a given duration of
 514 heating phase and concrete cover.

515 Figure 12 shows the CDF for the RC slab based on the actual and surrogate models. The
 516 estimated mean values for the minimum resisting moment of the slab during the parametric fire

517 exposure ('burnout' resistance; Gernay, 2019) based on 2000 and 100 LHS samples is
 518 approximately 27.27 kNm. Applying a direct evaluation of the 'actual model' the mean capacity
 519 of the slab is estimated as 27.28 kNm. Again, the fragility curve developed based on surrogate
 520 model agrees with that developed from the actual model, also for low capacity quantiles.



521
 522 Figure 12 Comparison of cumulative density function based on actual and surrogate model for
 523 RC slab under parametric fire ($\Gamma = 1$, $t_{\max} = 120$ min)

524 **4.2 Advanced non-linear model: Finite element evaluation of RC column load bearing**
 525 **capacity**

526 The surrogate model developed in Section 3.2 for the evaluation of the load bearing capacity
 527 (P_{\max}) of an RC column exposed to ISO 834 standard heating is adopted. Table 5 shows the
 528 stochastic variables, adopted from Van Coile et al. (2019). The fragility curve is developed
 529 based on 10^4 LHS samples of the stochastic variables as considered in earlier sections.

530
 531

532 Table 5 Probabilistic distributions for the model variables for the RC column exposed to ISO
 533 834 fire

Stochastic variables	Distribution	Mean	Standard deviation
Retention factor for yield strength of rebars, k_{fy} ($f_{yk,20} = 500$ MPa; $\mu_{fy,20} = 560$ MPa)	Logistic model (Qureshi et al., 2020)	Temperature-dependent	Temperature-dependent
Retention factor for concrete strength, f_c ($f_{ck,20} = 30$ MPa; $\mu_{fc,20} = 42.9$ MPa)			
Concrete cover, c	Beta [$\mu-3\sigma$; $\mu+3\sigma$]	47 mm	5 mm
Average eccentricity, e	Normal	0	0.004 m
Out of straightness, oos	Normal	0	0.004 m
Out of plumbness, oop	Normal	0	0.0015 rad

534 **4.2.1 Validation for probabilistic studies**

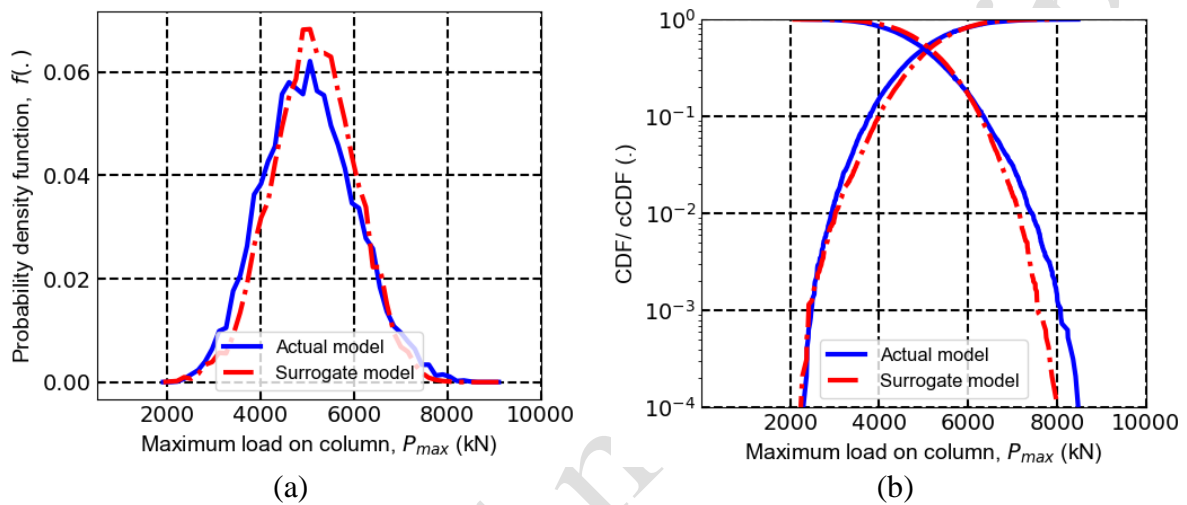
535 Figure 13(a) shows the comparison of the PDF evaluated by 10^4 evaluations of the actual and
 536 surrogate models. The PDFs from the two models agree reasonably well. The mean predicted
 537 capacity of the RC column after 4 hours of ISO 834 fire exposure based on actual and surrogate
 538 model are 5038 kN and 5137 kN, respectively. Similarly, the CDF based on surrogate model
 539 for the RC column is in good agreement with the CDF from the actual model, especially for
 540 low quantiles of P_{max} , as shown in Figure 13(b). As listed in Table 6, the 10^{-2} capacity quantile
 541 for the RC column is 2931 kN, which is predicted as 3010 kN (2.5 % error) through the
 542 surrogate model. From the perspective of computational expense, the probabilistic evaluation
 543 through the surrogate model was quasi-instantaneous, while the iterative evaluation of P_{max} in
 544 the actual model required multiple core-weeks on a modern PC (evaluation done through multi-
 545 processing in approximately 7 days).

546

Table 6 Capacity quantiles for RC column exposed to ISO 834 fire

S.N	CDF (.)	M_R of slab (kN) for RC column		Error (%)
		Surrogate model	Actual model	
1.	10^{-1}	3987	3805	4.7
2.	10^{-2}	3010	2931	2.70
3.	10^{-3}	2475	2414	2.52
4.	10^{-4}	2240	2300	2.60

547

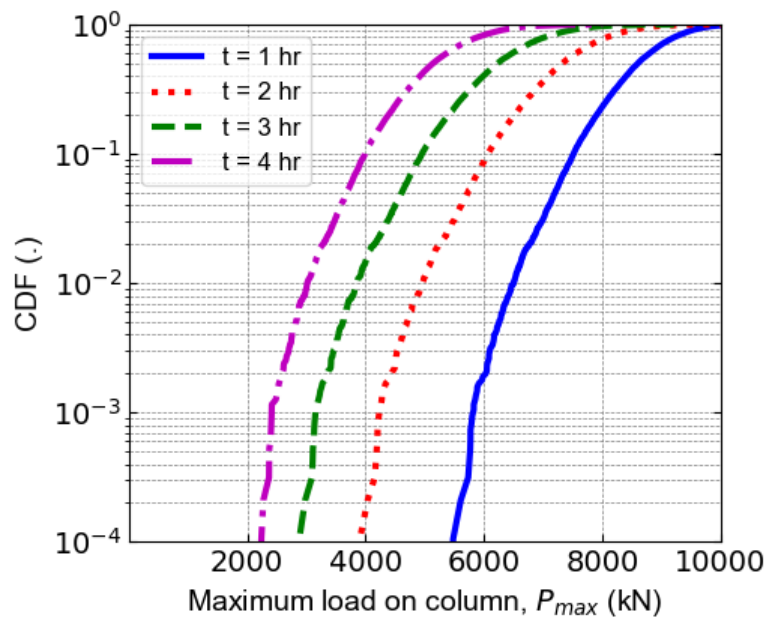


548 Figure 13 Comparison of (a) probability density function and (b) cumulative density function
 549 for RC column under 240 min of ISO 834 fire exposure

550 4.2.2 Generalized probabilistic evaluation

551 The evaluation of P_{max} through the actual model requires a computationally expensive iterative
 552 approach, see (Van Coile et al., 2020). This makes the updating of the probabilistic evaluation
 553 for design iterations impractical. Here, the surrogate model is applied to quasi-instantaneously
 554 perform probabilistic analyses for different ISO 834 exposure durations. Figure 14 shows
 555 obtained CDFs based on the surrogate model. The mean capacity of RC column after 1, 2, 3
 556 and 4 hr of standard fire exposure is estimated with the surrogate model as 8547 kN, 7290 kN,
 557 6210 kN and 5137 kN, respectively. Similarly, the 10^{-2} capacity quantile are 3010 kN, 3852
 558 kN, 4944 kN and 6513 kN. As the variable P_{max} relates to the load bearing capacity of the
 559 column, the results in Figure 14 can also be directly understood as fragility curves, where the

560 horizontal axis relates to the ‘intensity measure’ of total applied load. Such efficient generation
561 of fragility curves through surrogate modeling can be helpful in design iterations.



562

563 Figure 14 Cumulative density function for RC column exposed to different duration of ISO
564 834 fire

565 5 CONCLUSIONS

566 The potential of regression-based surrogate models for probabilistic studies of fire exposed
567 structure has been demonstrated. As a part of the proof-of-concept, the approach has been
568 applied to two structural fire engineering (SFE) models: (i) the bending moment capacity of a
569 concrete slab during fire, as defined by a simple analytical equation; and (ii) the load bearing
570 capacity of a concrete column during fire, considering an advanced numerical model. For both
571 cases, the fragility curves obtained through the surrogate model match with those obtained
572 through a direct application of the analytical/numerical model. The developed surrogate models
573 could predict the 10^{-2} capacity quantiles with an error of less than 5 %. A very significant
574 improvement in computational efficiency is observed. Furthermore, the surrogate modeling
575 methodology for probabilistic analysis has the important advantage that it can be applied to
576 quasi-instantaneously develop fragility curves considering modifications in the design or fire
577 scenarios, allowing probabilistic methods to be used as part of fast design iterations. It is

578 concluded that surrogate modelling approaches are particularly promising for probabilistic
579 structural fire engineering studies. As a next step in the application of surrogate models in SFE,
580 one suggestion is for surrogate models to be developed by interested individuals, industry
581 organizations, academic institutions and other. The latest surrogate models to be used by
582 practitioners can be made available in online repositories, with background to the model
583 training and validation made publicly available (e.g. through peer-reviewed journals).

584

585 REFERENCES

586 Baker, J. W., & Cornell, C. A. (2006). Vector-Valued Ground Motion Intensity Measures for
587 Probabilistic Seismic Demand Analysis. PEER Report 2006/08. *Pacific Earthquake*
588 *Engineering Research Center*. University of California, Berkeley.

589 Dexters A., Leisted R. R., Van Coile R., Welch S., Jomaas, G. (2019). Testing for Knowledge:
590 Maximising Information Obtained from Fire Tests by using Machine Learning Techniques.
591 *Proceedings of the 15th International Interflam conference*, 1.

592 Draper, N. R. and Smith, H. (1998). Applied Regression Analysis. *Wiley-Interscience*, 326

593 Du, S.S., Lee, J.D., Li, H., Wang, L. and Zhai, X., (2018). Gradient descent finds global minima
594 of deep neural networks. arXiv preprint arXiv:1811.03804.

595 EN 1991-1-2: 2002. Eurocode 1: actions on structures. General actions-actions on structures
596 exposed to fire.

597 EN 1992-1-2: 2004. Eurocode 2: design of concrete structures. General rules - Structural fire
598 design.

599 FEMA P58-1, (2012). Seismic Performance Assessment of Buildings: Volume 1—
600 Methodology.

601 Forrester, A., Sobester, A. and Keane, A., (2008). Engineering design via surrogate modelling:
602 a practical guide. *John Wiley & Sons*.

603 Franssen, J.M. and Gernay, T., (2017). Modeling structures in fire with SAFIR®: Theoretical
604 background and capabilities. *Journal of Structural Fire Engineering*, 8 (3), 300-323.

605 Fu, F., (2020). Fire induced progressive collapse potential assessment of steel framed buildings
606 using machine learning. *Journal of Constructional Steel Research*, 166, p.105918.

607 Gernay, T. (2019). Fire resistance and burnout resistance of reinforced concrete columns. *Fire*
608 *safety journal*, 104, 67-78.

609 Gernay, T., Khorasani, N. E., & Garlock, M. (2016). Fire fragility curves for steel buildings in
610 a community context: A methodology. *Engineering Structures*, 113, 259-276.

611 Gernay, T., Van Coile, R., Khorasani, N.E. and Hopkin, D., (2019a). Efficient uncertainty
612 quantification method applied to structural fire engineering computations. *Engineering*
613 *Structures*, 183, 1-17.

614 Gernay, T., Khorasani, N.E. and Garlock, M., (2019b). Fire fragility functions for steel frame
615 buildings: sensitivity analysis and reliability framework. *Fire Technology*, 55(4), pp.1175-
616 1210.

617 Guo, Q., Shi, K., Jia, Z., and Jeffers, A. E. (2013). Probabilistic evaluation of structural fire
618 resistance. *Fire technology*, 49(3), 793-811.

619 Guo, Q., & Jeffers, A. E. (2015). Finite-element reliability analysis of structures subjected to
620 fire. *Journal of Structural Engineering*, 141(4), 04014129.

621 Hamilton, S.R. (2011). Performance-based fire engineering for steel framed structures: a
622 probabilistic methodology. Doctoral dissertation. *Stanford University, USA*.

623 Hopkin, D., Van Coile, R., and Fu, I. (2018). Developing fragility curves and estimating failure
624 probabilities for protected steel structural elements subject to fully developed fires.
625 *Proceedings of the 10th International Conference on Structures in Fire*. 06-08/06, Belfast,
626 UK.

627 Hopkin, D., Van Coile, R., and Lange, D. (2017). Certain Uncertainty-Demonstrating safety in
628 fire engineering design and the need for safety targets. *SFPE Europe*.

629 Ioannou, I., Aspinall, W., Rush, D., Bisby, L., and Rossetto, T. (2017). Expert judgment-based
630 fragility assessment of reinforced concrete buildings exposed to fire. *Reliability Engineering
631 & System Safety*, 167, 105-127.

632 Ioffe, S. and Szegedy, C. (2015). Batch normalization: Accelerating deep network training by
633 reducing internal covariate shift. arXiv: 1502.03167.

634 ISO 24679-1:2019. Fire Safety Engineering – Performance of Structures in Fire – Part 1
635 General. *International Organization for Standardization*, Geneva, Switzerland.

636 ISO/CD TR 24679-8: 2020. Fire safety engineering — Performance of structures in fire — Part
637 8: Example of a probabilistic fire design of structures.

638 James, G., Witten, D., Hastie, T. and Tibshirani, R., (2013). An introduction to statistical
639 learning. *New York: springer*, 112, 3-7..

640 JCSS. (2013). Probabilistic Model Code. Joint Committee on Structural Safety. Available
641 online at <http://www.jcss.byg.dtu.dk/>

642 Khorasani, N. E., Gardoni, P., and Garlock, M. (2015). Probabilistic fire analysis: material
643 models and evaluation of steel structural members. *Journal of Structural Engineering*,
644 141(12), 04015050.

645 Lange, D., Devaney, S., & Usmani, A. (2014). An application of the PEER performance based
646 earthquake engineering framework to structures in fire. *Engineering structures*, 66, 100-115.

647 McNamee, M., Meacham, B., van Hees, P., Bisby, L., Chow, W. K., Coppalle, A., ... & Floyd,
648 J. (2019). IAFSS agenda 2030 for a fire safe world. *Fire Safety Journal*, 110, 102889.

649 Naser, M. Z., (2019a). Fire resistance evaluation through artificial intelligence-A case for
650 timber structures. *Fire safety journal*, 105, 1-18.

651 Naser, M. Z. (2019b). Can past failures help identify vulnerable bridges to extreme events? A
652 biomimetical machine learning approach. *Engineering with Computers*, 1-33.

653 Olsson, A., Sandberg, G. and Dahlblom, O., (2003). On Latin hypercube sampling for structural
654 reliability analysis. *Structural safety*, 25(1), 47-68.

655 Panev, Y., Kotsovinos, P., Deeny, S., & Flint, G. (2021). The Use of Machine Learning for the
656 Prediction of fire Resistance of Composite Shallow Floor Systems. *Fire Technology*, 1-22.

657 Qureshi, R., Ni, S., Elhami Khorasani, N., Van Coile, R., Hopkin, D. and Gernay, T., (2020).
658 Probabilistic Models for Temperature-Dependent Strength of Steel and Concrete. *Journal of*
659 *Structural Engineering*, 146(6), 04020102.

660 Rudin, C., (2019). Stop explaining black box machine learning models for high stakes decisions
661 and use interpretable models instead. *Nature Machine Intelligence*, 1(5), 206-215.

662 Seitlari, A. and Naser, M.Z., (2019). Leveraging artificial intelligence to assess explosive
663 spalling in fire-exposed RC columns. *Computers and Concrete*, 24(3), 271-282.

664 Shrivastava, M., Abu, A. K., Dhakal, R. P., and Moss, P. J. (2019). Severity measures and stripe
665 analysis for probabilistic structural fire engineering. *Fire Technology*, 55(4), 1147-1173.

666 Spinardi, G., Bisby, L. and Torero, J., (2017). A review of sociological issues in fire safety
667 regulation. *Fire Technology*, 53(3), 1011-1037.

668 Thienpont, T., Van Coile, R., Caspeepe, R. and De Corte, W. (2019). Comparison of fire re-
669 sistance and burnout resistance of simply supported reinforced concrete slabs exposed to
670 parametric fires. *In 3rd International Conference on Structural Safety under Fire and Blast*.

671 Van Coile, R., Caspeepe, R. and Taerwe, L. (2013). The mixed lognormal distribution for a
672 more precise assessment of the reliability of concrete slabs exposed to fire. *In Proceedings*
673 *of ESREL*, 2013, 29(09), 02-10.

674 Van Coile, R., Caspeepe, R., and Taerwe, L. (2014). Reliability-based evaluation of the inherent
675 safety presumptions in common fire safety design. *Engineering structures*, 77, 181-192.

676 Van Coile, R., Hopkin, D., Lange, D., Jomaas, G., and Bisby, L. (2019). The need for
677 hierarchies of acceptance criteria for probabilistic risk assessments in fire engineering. *Fire*
678 *Technology*, 55(4), 1111-1146.

679 Van Coile, R., Hopkin, D., Elhami Khorasani, N. and Gernay, T., (2020). Demonstrating
680 adequate safety for a concrete column exposed to fire, using probabilistic methods. *Fire and*
681 *Materials*. <https://doi.org/10.1002/fam.2835>.

682 Virtanen, P., Gommers, R., Oliphant, T.E., Haberland, M., Reddy, T., Cournapeau, D.,
683 Burovski, E., Peterson, P., Weckesser, W., Bright, J. and van der Walt, S.J., (2020). SciPy
684 1.0: fundamental algorithms for scientific computing in Python. *Nature methods*, 17(3), 261-
685 272.

686

687

688

689

690 **Annex:** Evaluation of concrete slab bending capacity for known rebar temperature (Simple non-
691 linear model)

692

693 Table 1 Regression coefficients, with mean and standard deviation of polynomial terms of the
694 surrogate model ($m=2$)

S.N	Polynomial terms, c	Dimension	Regression coefficients, θ	Mean, μ_c	Standard deviation, σ_c
0.	Bias	-	6.01E-15	1.00E+00	0.00E+00
1.	$f_{c,20^\circ C}$	N/m ²	-1.66E-02	4.75E+01	1.88E+01
2.	$f_{c,20^\circ C}^2$	N ² /m ⁴	-3.03E-02	2.61E+03	1.81E+03
3.	$f_{c,20^\circ C} \times f_{y,T}$	N ² /m ⁴	2.62E-02	2.61E+04	1.68E+04
4.	$f_{c,20^\circ C} \times c$	N/m	-4.10E-03	2.19E+00	1.05E+00
5.	$f_{c,20^\circ C} \times h$	N/m	-1.008E-02	9.52E+00	4.81E+00
6.	$f_{c,20^\circ C} \times A_s$	N	6.26E-02	1.90E-02	8.06E-03
7.	$f_{y,T}$	N/m ²	-5.47E-01	5.50E+02	2.60E+02
8.	$f_{y,T}^2$	N ² /m ⁴	-3.46E-02	3.70E+05	2.92E+05
9.	$f_{y,T} \times c$	N/m	-2.601E-01	2.53+01	1.39E+01
10.	$f_{y,T} \times h$	N/m	1.14E+00	1.10E+02	6.24E+01
11.	$f_{y,T} \times A_s$	N	5.83E-01	2.20E-01	1.10E-01
12.	c	m	1.50E-01	4.60E-02	1.15E-02
13.	c^2	m ²	9.15E-03	2.25E-03	1.07E-03
14.	$c \times h$	m ²	-3.67E-02	9.20E-03	3.57E-03
15.	$(c \times A_s)$	m ³	-1.53E-01	1.84E-05	5.38E-06
16.	h	m	-4.57E-01	2.00E-01	5.77E-02
17.	h^2	m ²	5.76E-03	4.33E-02	2.33E-02
18.	$(h \times A_s)$	m ³	5.54E-01	8.00E-05	2.60E-05
19.	A_s	m ²	-1.25E-01	4.00E-04	5.77E-05
20.	A_s^2	m ⁴	-2.08E-02	1.63E-07	4.63E-08

695

696 The surrogate model was trained for normalized model output, with $\mu_{MR} = 330743$ Nm and σ_{MR}
697 = 21605 Nm. Based on the above Table, the moment capacity of slab can be estimated as:

$$698 \quad M_R [Nm] = \left(\theta_0 + \sum_{i=1}^{20} \left(\frac{c_i - \mu_i}{\sigma_i} \right) \theta_i \right) 21605 + 330743$$

699